

## VU Research Portal

### Multiple and dependent scattering effects in Doppler optical coherence tomography

Kalkman, J.; Bykov, A.J.; Faber, D.J.; van Leeuwen, T.G.

**published in**  
Optics Express  
2010

**DOI (link to publisher)**  
[10.1364/OE.18.003883](https://doi.org/10.1364/OE.18.003883)

**document version**  
Publisher's PDF, also known as Version of record

[Link to publication in VU Research Portal](#)

#### **citation for published version (APA)**

Kalkman, J., Bykov, A. J., Faber, D. J., & van Leeuwen, T. G. (2010). Multiple and dependent scattering effects in Doppler optical coherence tomography. *Optics Express*, 18(4), 3883-3892.  
<https://doi.org/10.1364/OE.18.003883>

#### **General rights**

Copyright and moral rights for the publications made accessible in the public portal are retained by the authors and/or other copyright owners and it is a condition of accessing publications that users recognise and abide by the legal requirements associated with these rights.

- Users may download and print one copy of any publication from the public portal for the purpose of private study or research.
- You may not further distribute the material or use it for any profit-making activity or commercial gain
- You may freely distribute the URL identifying the publication in the public portal ?

#### **Take down policy**

If you believe that this document breaches copyright please contact us providing details, and we will remove access to the work immediately and investigate your claim.

**E-mail address:**  
[vuresearchportal.ub@vu.nl](mailto:vuresearchportal.ub@vu.nl)

# Multiple and dependent scattering effects in Doppler optical coherence tomography

J. Kalkman<sup>1,\*</sup>, A. V. Bykov<sup>2</sup>, D. J. Faber<sup>1,3</sup>, and T. G. van Leeuwen<sup>1,4</sup>

<sup>1</sup>Biomedical Engineering & Physics, Academic Medical Center, University of Amsterdam, PO Box 22700, 1100 DE Amsterdam, The Netherlands

<sup>2</sup>Optoelectronics and Measurement Techniques Laboratory, University of Oulu, PO Box 4500, 90014 Oulu, Finland

<sup>3</sup>Ophthalmology Department, Academic Medical Center, University of Amsterdam, PO Box 22700, 1100 DE Amsterdam, The Netherlands

<sup>4</sup>Biomedical Photonic Imaging, MIRA Institute for Biomedical Technology and Technical Medicine, University of Twente, PO Box 217, 7500 AE Enschede, The Netherlands

[\\*j.kalkman@amc.nl](mailto:*j.kalkman@amc.nl)

**Abstract:** Doppler optical coherence tomography (OCT) is a technique to image tissue morphology and to measure flow in turbid media. In its most basic form, it is based on single (Mie) scattering. However, for highly scattering and dense media multiple and concentration dependent scattering can occur. For Intralipid solutions with varying scattering strength, the effect of multiple and dependent scattering on the OCT signal attenuation and Doppler flow is investigated. We observe a non-linear increase in the OCT signal attenuation rate and an increasingly more distorted Doppler OCT flow profile with increasing Intralipid concentration. The Doppler OCT attenuation and flow measurements are compared to Monte Carlo simulations and good agreement is observed. Based on this comparison, we determine that the single scattering attenuation coefficient  $\mu_s$  is 15% higher than the measured OCT signal attenuation rate. This effect and the distortion of the measured flow profile are caused by multiple scattering. The non-linear behavior of the single scattering attenuation coefficient with Intralipid concentration is attributed to concentration dependent scattering.

©2010 Optical Society of America

**OCIS codes:** (170.4500) Optical coherence tomography; (170.3880) Medical and biological imaging; (290.4210) Multiple scattering; (290.7050) Turbid media.

---

## References

1. Z. Chen, T. E. Milner, D. Dave, and J. S. Nelson, "Optical Doppler tomographic imaging of fluid flow velocity in highly scattering media," *Opt. Lett.* **22**(1), 64–66 (1997).
2. J. A. Izatt, M. R. Hee, G. M. Owen, E. A. Swanson, and J. G. Fujimoto, "Optical coherence microscopy in scattering media," *Opt. Lett.* **19**(8), 590–592 (1994).
3. L. Thrane, H. T. Yura, and P. E. Andersen, "Analysis of optical coherence tomography systems based on the extended Huygens–Fresnel principle," *J. Opt. Soc. Am. A* **17**(3), 484 (2000).
4. D. J. Faber, and T. G. van Leeuwen, "Are quantitative attenuation measurements of blood by optical coherence tomography feasible?" *Opt. Lett.* **34**(9), 1435–1437 (2009).
5. R. K. Wang, "Signal degradation by multiple scattering in optical coherence tomography of dense tissue: a Monte Carlo study towards optical clearing of biotissues," *Phys. Med. Biol.* **47**(13), 2281–2299 (2002).
6. H. T. Yura, L. Thrane, and P. E. Andersen, "Analysis of multiple scattering effects in optical Doppler tomography," *Proc. SPIE* **5861**, 5861B–1 (2005).
7. A. V. Bykov, M. Yu. Kirillin, and A. V. Priezhev, "Monte Carlo simulation of an optical coherence Doppler tomography signal: the effect of the concentration of particles in a flow on the reconstructed velocity profile," *Quantum Electron.* **35**(2), 135–139 (2005).
8. J. Moger, S. J. Matcher, C. P. Winlove, and A. Shore, "The effect of multiple scattering on velocity profiles measured using Doppler OCT," *J. Appl. Phys. D.* **38**(15), 2597–2605 (2005).
9. T. G. van Leeuwen, M. D. Kulkarni, S. Yazdanfar, A. M. Rollins, and J. A. Izatt, "High-flow-velocity and shear-rate imaging by use of color Doppler optical coherence tomography," *Opt. Lett.* **24**(22), 1584–1586 (1999).
10. G. Göbel, J. Kuhn, and J. Fricke, "Dependent scattering effects in latex-sphere suspensions and scattering powders," *Waves Random Complex Media* **5**(4), 413–426 (1995).

11. G. Zaccanti, S. Del Bianco, and F. Martelli, "Measurements of optical properties of high-density media," *Appl. Opt.* **42**(19), 4023–4030 (2003).
12. T. G. van Leeuwen, D. J. Faber, and M. C. Aalders, "Measurement of the axial point spread function in scattering media using single-mode fiber-based optical coherence tomography," *IEEE J. Sel. Top. Quantum Electron.* **9**(2), 227–233 (2003).
13. H. J. van Staveren, C. J. M. Moes, J. van Marle, S. A. Prahl, and M. J. C. van Gemert, "Light scattering in Intralipid-10% in the wavelength range of 400–1100 nm," *Appl. Opt.* **30**(31), 4507 (1991).
14. R. Michels, F. Foschum, and A. Kienle, "Optical properties of fat emulsions," *Opt. Express* **16**(8), 5907 (2008).
15. D. J. Faber, F. J. van der Meer, M. C. G. Aalders, and T. G. van Leeuwen, "Quantitative measurement of attenuation coefficients of weakly scattering media using optical coherence tomography," *Opt. Express* **12**(19), 4353–4365 (2004).
16. K. F. Palmer, and D. Williams, "Optical properties of water in the near infrared," *J. Opt. Soc. Am.* **64**(8), 1107 (1974).
17. L. Wang, Y. Wang, S. Guo, J. Zhang, M. Bachman, G. P. Li, and Z. Chen, "Frequency domain phase-resolved optical Doppler and Doppler variance tomography," *Opt. Commun.* **242**(4–6), 345–350 (2004).
18. E. Koch, J. Walther, and M. Cuevas, "Limits of Fourier domain Doppler-OCT at high velocities," *Sens. Actuators A* **156**(1), 8–13 (2009).
19. M. Szkulmowski, A. Szkulmowska, T. Bajraszewski, A. Kowalczyk, and M. Wojtkowski, "Flow velocity estimation using joint Spectral and Time domain Optical Coherence Tomography," *Opt. Express* **16**(9), 6008–6025 (2008).
20. A. V. Bykov, M. Yu. Kirillin, and A. V. Priezzhev, "Analysis of distortions in the velocity profiles of suspension flows inside a light-scattering medium upon their reconstruction from the optical coherence Doppler tomography signal," *Quantum Electron.* **35**(11), 1079–1082 (2005).
21. H. Ren, T. Sun, D. J. MacDonald, M. J. Cobb, and X. Li, "Real-time in vivo blood-flow imaging by moving-scatterer-sensitive spectral-domain optical Doppler tomography," *Opt. Lett.* **31**(7), 927–929 (2006).
22. A. Ishimaru, and Y. Kuga, "Attenuation constant of a coherent field in a dense distribution of particles," *J. Opt. Soc. Am.* **72**(10), 1317 (1982).
23. B. L. Drolen, and C. L. Tien, "Independent and dependent scattering in packed-sphere systems," *Int. J. Thermophys.* **1**(1), 63–68 (1987).

## 1. Introduction

Doppler optical coherence tomography (OCT) is a well established technique for the simultaneous imaging of static and moving components in near-surface regions of biological tissues [1]. By coherent gating, OCT performs a path length resolved measurement of the photons scattered from tissue. The use of coherent gating in combination with confocal light collection significantly reduces the number of detected multiple scattered photons, thereby increasing the imaging depth by a factor three compared to confocal microscopy [2]. Determination of the tissue scattering coefficient, quantitative depth ranging, and flow measurement with Doppler OCT are generally based on single backscattering. For example, in case only single scattering and no absorption is present, the OCT signal attenuation rate is equal to the scattering coefficient  $\mu_s$ . However, for highly scattering media and due to the finite collection numerical aperture and coherence length, multiple scattered photons are also present in the OCT signal, thereby changing the measured OCT signal attenuation. In addition, multiple scattering can lead to non single-exponential decay, thereby making a quantitative determination of the scattering coefficient more difficult [3,4]. Moreover, since in OCT the path length of the detected photons is mapped one on one to a geometrical location in the sample, multiple scattering can also affect depth ranging, and it can lead to spatial resolution loss [5]. For Doppler OCT flow measurements it has been shown theoretically [6], with Monte Carlo (MC) simulations [7], and experimentally [8] that multiple scattering can increase or decrease the Doppler frequency for light penetrating deep into highly scattering media. Consequently, for a quantitative analysis of Doppler OCT data, e.g. to correctly determine flow and/or shear rate parameters [9], the effect of multiple scattering has to be taken into account.

In addition to multiple scattering, the scattering coefficient is also influenced by coherent light scattering effects, i.e. due to close packing of particles the coherent addition of light can lead to a reduction in the scattering rate. This effect is called dependent scattering; a dependence of the scattering strength on the separation between the particles. In this case the scattering coefficient  $\mu_s$  does not follow the linear relation  $\mu_s = C\sigma_s$ , but instead the Mie scattering cross section  $\sigma_s$  depends in a complex way on particle concentration  $C$  and therefore the relation

$\mu_s = C\sigma_s(C)$  holds. As already shown in other light scattering experiments [10,11] dependent scattering leads to a reduction in the scattering rate can thus lead to a decrease of the OCT signal attenuation.

Here, we present Doppler OCT measurements on Intralipid solutions under flow. The Intralipid solutions have varying scattering strength. The Doppler OCT attenuation and flow profiles are compared to MC simulations. The effects of multiple and dependent scattering in Intralipid on the OCT signal attenuation and Doppler profile are separated and quantified.

## 2. Materials and methods

### 2.1 Doppler Optical Coherence Tomography

The OCT experiments are conducted on a home-built spectral-domain OCT system based on single mode fibers (SMF-28). A schematic of the set-up can be seen in Fig. 1. The light source is a B&W Tek superluminescent diode light source with 7 mW output power, 40 nm optical bandwidth, and a center wavelength of  $\lambda_c = 1300$  nm. Via a circulator the light is coupled into a 90/10 beamsplitter, we have 4.5 mW output power at the sample for all measurements. There are polarization controllers in both sample (90%) and reference arm (10%). An XY scanner is mounted on the sample arm and with a lens ( $NA = 0.02$ ) the light is focused at 250 micron below the zero delay point. The zero delay point is 200  $\mu\text{m}$  in front of the scattering medium. The back reflected light is redirected through the optical circulator to the spectrometer. The spectrometer consists of an achromatic collimator lens ( $f = 70$  mm) that directs the beam on a volume transmission grating (Wasatch Photonics, 1145 lines/mm). The collimated beam is imaged with a lens doublet, consisting of an achromatic focusing lens ( $f = 400$  mm) and a singlet lens ( $f = 150$  mm), onto a 46 kHz CCD linescan camera (Sensors Unlimited SU-LDH-1.7RT/LC). In software, the acquired spectra are processed in the following order: 1) reference arm spectrum subtraction 2) dispersion compensation 3) spectral resampling to k-space.

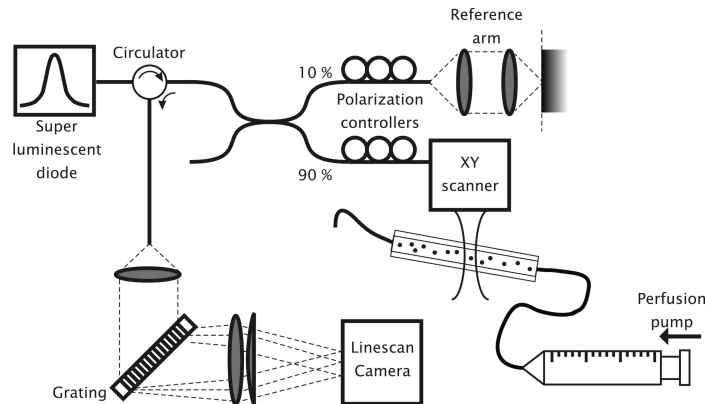


Fig. 1. Schematic overview of the spectral-domain Doppler OCT set-up used in the experiments. Doppler OCT measurements are performed without scanning the beam. More details about the various OCT components can be found in the text.

We achieve a depth resolution of 18  $\mu\text{m}$  and a maximum sensitivity of  $-97$  dB (both measured at 200  $\mu\text{m}$  depth). The OCT 6 dB signal roll-off point is at 1500  $\mu\text{m}$  depth. A-line measurements are performed at the maximum line rate; 1056 A-lines are averaged per measurement. The measured OCT signal amplitude is corrected for the confocal point spread function [12] and the system depth sensitivity. Optical path lengths are converted to physical depth by dividing the optical path length with an effective index based on the particle ( $n = 1.46$ , soybean oil) and water volume fraction ( $n = 1.32$ ) [13,14]. The OCT signal attenuation coefficient is determined by a 2-parameter single exponential fit (attenuation rate and amplitude) over the region of the cuvette. It has been shown that this is a simple and valid

model for the OCT signal attenuation [15]. The fitted attenuation coefficient is converted to  $\mu_s$  by subtracting the Intralipid concentration dependent optical absorption ( $0.136 \text{ mm}^{-1}$  at 1300 nm wavelength for water [16] and negligible for the solid part of the Intralipid).

The phase stability of the OCT system is measured from the peak of a single mirror reflection and is 1 degree per 16 ms. The Doppler frequency is determined by calculating the incremental phase change per A-line [17]. The measured Doppler flow profiles are fitted between the boundaries of the cuvette with two models. First, a 1-parameter parabolic flow model:  $V(d) = V_{\max}(1-(d/r)^2)$ , with  $V_{\max}$ , the maximum amplitude of the flow,  $d$  the depth calculated from the glass/Intralipid interface and  $r$  is one half of the cuvette channel width. Second, a 3-parameter non-symmetric fit model that consists of a parabola and additional polynomial terms:  $V(d) = V_{\max}(1-(d/r)^2) + \alpha d + \beta d^3$ , with  $V_{\max}$ ,  $\alpha$ , and  $\beta$  fit parameters. The measurement and fitting procedure of the OCT attenuation and Doppler OCT flow are repeated five times for every Intralipid concentration to calculate the standard deviation of the measured scattering coefficient and of the fit parameters of the Doppler OCT flow profile.

As a scattering medium we use dilutions of a single batch of 20 weight% Intralipid (Fresenius-Kabi) with distilled water. The Intralipid (particle) volume concentration is calculated by assuming that only the soy-bean oil and the eggphospholipid are in the solid state, with the rest of the constituents (glycerol and water) in solution [14]. Flow is generated by a precision syringe pump (Perfusor fm, B. Braun AG) that pumps the Intralipid solution at a flow of 50 ml/h through a 500  $\mu\text{m}$  thickness glass flow cuvette ( $n = 1.43$ ). The glass flow cuvette is mounted at an angle of  $71.6 \pm 0.7$  degrees relative to the incoming beam. The measured flow fluctuates slowly with  $\sim 10\%$  in time. For this flow rate and Doppler angle we obtain a laminar flow with a Doppler frequency far below the maximum Doppler frequency ( $<13\%$  of half the maximum A-line rate) to avoid phase-wrapping, non-linear effects [18], and/or an underestimation of the flow [19].

## 2.2 Monte Carlo simulations

MC simulations are performed using a parallel (message passing interface based) MC code for light propagation in multilayered scattering media [20] using a computer cluster system based on Intel Xeon 3 GHz processors. For the calculation of a single OCT A-line the trajectories of  $10^{11}$  photons are generated and analyzed. The incoming photons are modeled in the form of a pencil beam. Photons are assumed coherent if their single pass optical pathlength is within half a coherence length of their maximum depth (weighted by a Gaussian). The outgoing coherent photons are detected using a Gaussian beam geometry finite size detector located at the focal distance from the medium under study. More details on the MC code and the OCT signal simulation can be found in Ref [7]. The experimental conditions are matched by taking the parameters as shown in Fig. 2. The Intralipid is modeled by parameters  $\mu_s$ ,  $\mu_a$ , and the scattering anisotropy  $g$ . For the scattering coefficient the experimentally measured scattering coefficient  $\mu_s$  is used, thereby taking dependent scattering into account. For the absorption coefficient  $\mu_a$ , the water concentration dependent absorption is calculated (see section 2.1). In the calculations we neglect any effect of the varying Intralipid concentration on the coherence length (through absorption and refractive index) and on the scattering anisotropy.

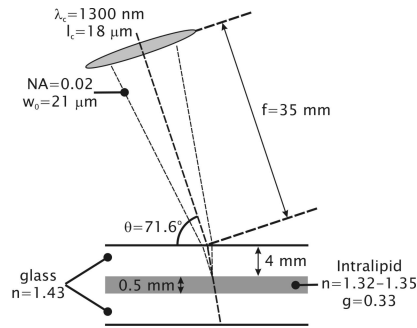


Fig. 2. Schematic overview of the MC simulation parameters. The coherence length of the source is given by  $l_c$ , the Gaussian beam waist at the focal position is given by  $w_0$ .

### 3. Results

#### 3.1 OCT signal attenuation

Figure 3(a) shows a single average A-line OCT measurement (no lateral scanning) for three different Intralipid solutions during flow. The data are plotted with OCT amplitude on a logarithmic scale, with an offset between the different measurements to facilitate a comparison. As can be seen, the OCT signal attenuates more or less as a single exponential over the full depth of the cuvette for all Intralipid concentrations. From a single exponential fit to the data (assuming single scattering only) the scattering coefficient  $\mu_s$  is determined and plotted against Intralipid (particle) volume concentration in Fig. 3(b). Interestingly, instead of the expected linear increase of  $\mu_s$  with Intralipid concentration, we observe a strong non-linear increase of  $\mu_s$  with increasing Intralipid concentration. The OCT attenuation coefficient saturates at  $\sim 5 \text{ mm}^{-1}$  for 23 vol.% Intralipid.

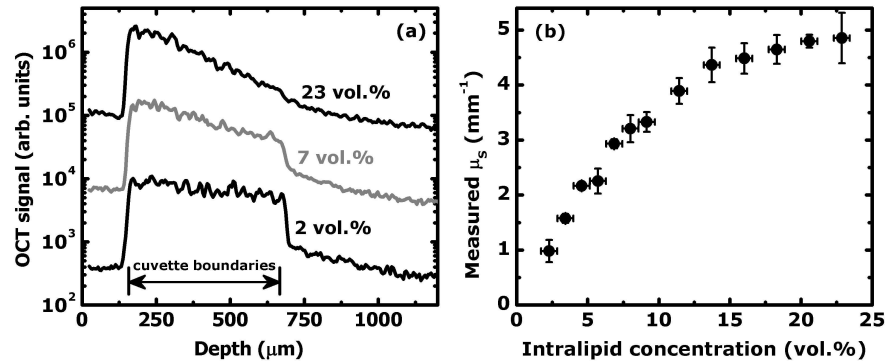


Fig. 3. (a) OCT signal attenuation versus depth for varying Intralipid concentration. (b) Measured average scattering coefficient  $\mu_s$  for varying Intralipid concentration ( $\mu_s$  data obtained from the OCT signal slope is corrected for water absorption). The error bars depict the standard deviation of the measurement ( $N = 5$ ).

#### 3.2 Doppler OCT signal

Figure 4 shows single average Doppler OCT profiles, which are measured simultaneously with the attenuation measurements presented in Fig. 3(a). As expected, for low Intralipid concentration, the flow profile between the borders of the cuvette is a parabola; however the parabolic flow profile becomes strongly asymmetric for higher Intralipid concentrations. This effect can be most clearly seen at the deepest cuvette wall (second minimum of the parabola). At this position the flow boundary condition requires the flow to be zero, which indeed would have been measured in case only single scattering is present. Instead, the Doppler frequency at the deepest cuvette wall increases with increasing Intralipid concentration. We attribute this to

multiple scattering, where photons with a pathlength equal to the single backscattered photons are also detected, but where these photons have experienced multiple scattering events. Consequently, the average Doppler frequency of the photons with this pathlength increases.

For higher Intralipid concentrations the phase noise in the Doppler signal increases for larger depths. However, since the flow cuvette is thin, the signal to noise ratio is relatively high for all depths. Therefore, the phase noise fluctuations are relatively small and we can accurately determine the Doppler frequency for all depths and for all Intralipid concentrations. In addition, we have also observed the same deviations in the measured flow profile with the zero-delay point at the back of the cuvette. In this case the signal to noise ratio is much higher for the larger depths and any effect of a reduced signal to noise ratio is much smaller.

Doppler OCT signals also can be observed for depths less than 150  $\mu\text{m}$  and larger than 670  $\mu\text{m}$ . For these depths there are no scatterers present in the sample and therefore these signals are measurement artifacts. Both artifact signals are absent when the reference arm is blocked. The shallower depths are attributed to the DC background signal in the OCT measurement, which is Doppler shifted (see Fig. 3(a)). The larger depths are attributed to multiple scattering in the cuvette resulting in optical paths that are longer than the cuvette length. From the OCT signal at these depths and the noise in the Doppler OCT data it can be observed that these signals are caused by very few photons on the detector. For blood a similar effect was observed, see Ref [8]. In many cases in literature these signals are removed from the Doppler measurement by thresholding the Doppler OCT data with the OCT signal magnitude (e.g. see Ref [21].).

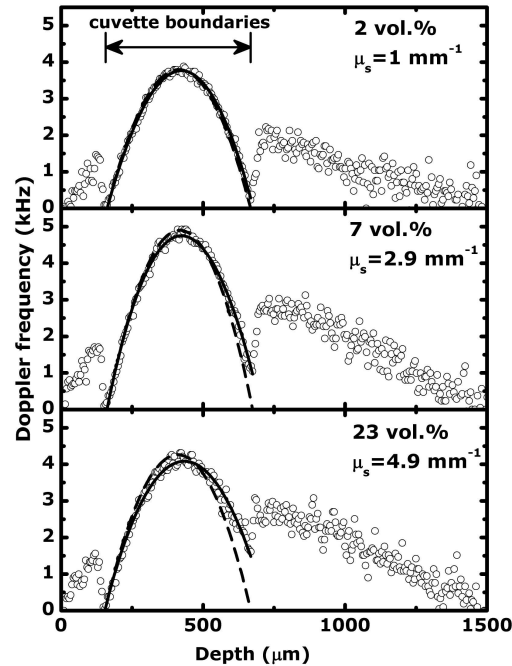


Fig. 4. Doppler OCT measurement for three Intralipid concentrations with the measured  $\mu_s$  indicated. The flow profile is fitted between the boundaries of the cuvette (minima of the flow profile) with two models; the fit functions are shown in the graph. Doppler OCT signal artifacts can be observed for depths smaller than 150  $\mu\text{m}$  and larger than 670  $\mu\text{m}$ .

To facilitate a quantitative analysis of the measured Doppler OCT flow, the flow profiles are fitted with two models. As can be clearly observed in Fig. 4, for low Intralipid concentrations, both the 1-parameter parabola model and the 3-parameter model yield a good fit to the data. For the higher Intralipid concentrations the 1-parameter model shows a poor fit, whereas the 3-parameter model fits well to the data, clearly demonstrating the asymmetry of the measured

flow profile. From the fits to the data we can quantify three effects of multiple scattering on the measured Doppler OCT flow profile for increasing Intralipid concentration:

- 1) the measured position of the peak of the flow velocity shifts to a larger depth;  $(8 \pm 2)\%$  increase relative to the center for 23 vol.% Intralipid
- 2) the measured flow velocity increases at the back end of the cuvette;  $(40 \pm 3)\%$  of the measured peak flow for 23 vol.% Intralipid
- 3) the peak flow velocity of the 1-parameter parabolic fit overestimates the measured Doppler peak flow;  $(5.3 \pm 0.6)\%$  for 23 vol.% Intralipid

### 3.3 Monte Carlo simulation of the OCT signal attenuation

To determine the interplay between multiple and dependent scattering on the Doppler OCT signal, we compare the experimental results with MC simulations. Figure 5 shows the simulated OCT signal as a function of depth, with the measured  $\mu_s$  for three Intralipid concentrations as input ( $\mu_a = 0$ ). As can be seen, the simulated OCT signal decay is close to the expected scattering coefficient  $\mu_s$ , but for all Intralipid concentrations the slope of the single exponential part of the simulated OCT attenuation is slightly lower than the input  $\mu_s$  ( $\sim 13\%$ ), as indicated on the right hand side of Fig. 5. The construction of the OCT signal is clarified by sorting the detected photons into different classes related to the number of scattering events per photon.

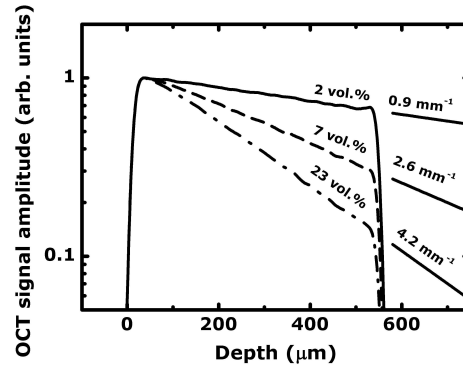


Fig. 5. Monte Carlo simulations of the OCT signal attenuation in depth for varying Intralipid concentration. The simulations are performed with  $\mu_s = 1, 2.9, 4.9 \text{ mm}^{-1}$ , for 2, 7, and 23 vol.% Intralipid, respectively. Indicated on the right are the effective OCT attenuation coefficients obtained for these simulations.

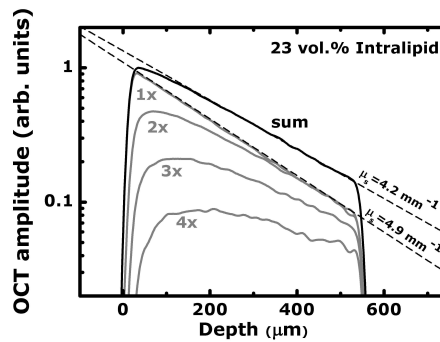


Fig. 6. Monte Carlo simulation of the OCT signal attenuation for 23 vol.% Intralipid. The sum of the OCT signal is decomposed into classes related to the number of scattering events per photon (indicated). For single backscattering the attenuation is equal to the input  $\mu_s$ . Multiple scattering adds signal to the OCT signal amplitude thereby decreasing the scattering coefficient from  $\mu_s = 4.9 \text{ mm}^{-1}$  to  $4.2 \text{ mm}^{-1}$ .



Figure 6 shows the construction of the OCT signal attenuation for 23 vol.% Intralipid in more detail. As can be seen, the single (back) scattered photons have an attenuation of  $\mu_s$ , as expected. Yet, due to the finite collection numerical aperture and coherence length, multiple scattered photons are also detected. For depths larger than 200  $\mu\text{m}$  the number of multiple scattered photons (scattered more than  $1 \times$ ) exceeds the number of single scattered photons, and since multiple scattered photons are found to have a lower attenuation rate with depth, their addition to the single backscattered photons leads to a decrease of the attenuation rate compared to  $\mu_s$ . Therefore the OCT signal attenuation becomes slightly non single exponential as it changes from mainly single backscattering (depth  $< 200 \mu\text{m}$ ) to mainly multiple scattered (depth  $> 200 \mu\text{m}$ ). With some difficulty, the non single exponential attenuation can be observed in the experimental data, however due to experimental inaccuracies from the point spread function correction and fluctuations of the signal (see the vertical error bars in Fig. 3(b)) we could not quantify the non single-exponential OCT attenuation in our measurements. Nevertheless, we achieved a relatively good single-exponential fit for all Intralipid concentrations. From the MC simulations we derive that the measured OCT signal attenuation slope is  $\sim 87\%$  of the single scattering coefficient. The single scattering coefficient  $\mu_s$  is thus  $0.87^{-1} = 1.15$  times higher than the values shown in Fig. 3(b).

### 3.4 Monte Carlo simulation of the Doppler OCT signal

Next, we perform MC simulations of the Doppler OCT signal, and include  $\mu_a$  in the MC simulations. The input  $\mu_s$  for the MC simulation is increased with 15% relative to the measured  $\mu_s$  so that the simulated OCT signal attenuation rate is in agreement with the experimentally determined scattering coefficient (see Fig. 5). Figure 7 shows the simulated OCT Doppler signal for three different Intralipid concentrations with a normalized input flow. It demonstrates that for increasing Intralipid concentration the flow maximum shifts to a larger depth (+ 9% relative to the center) and that the Doppler frequency at the back end of the cuvette increases (+ 40% of the peak flow), both are observed in our measurements. Also, the peak flow decreases. This effect is difficult to observe in our measurements due to the flow variations of the syringe pump, dependence of the Doppler frequency on the refractive index of the Intralipid, and incidence angle variations due to the refractive index of the Intralipid. As expected, for single scattered photons the simulated Doppler flow profile is equal to the input parabolic flow profile (not shown).

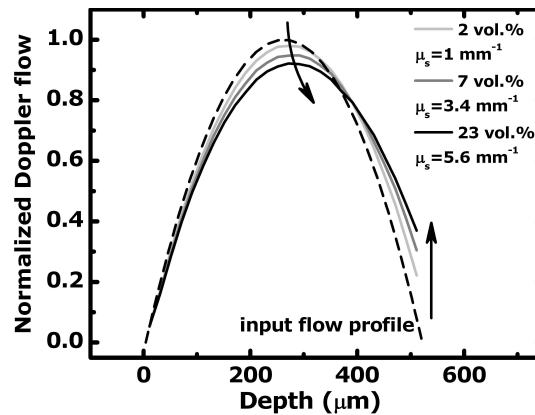


Fig. 7. Monte Carlo simulation of the Doppler OCT signal for varying Intralipid concentration (indicated). The input flow profile is indicated by the dashed line. The effects of increasing amounts of multiple scattering are indicated by the arrows. They are: a decrease of the measured peak flow, a shift of the measured peak flow to a larger depth, and an increase of the measured flow deeper into the sample.

The Doppler frequency MC simulations are compared to the experimental OCT data in Fig. 8. Both the experimental data and the simulated Doppler frequency data are normalized. Figure 8 shows the good agreement between the MC simulation and the measurements. Especially the offset of the flow at the deepest cuvette wall increases with Intralipid concentration in accordance with the measurements.

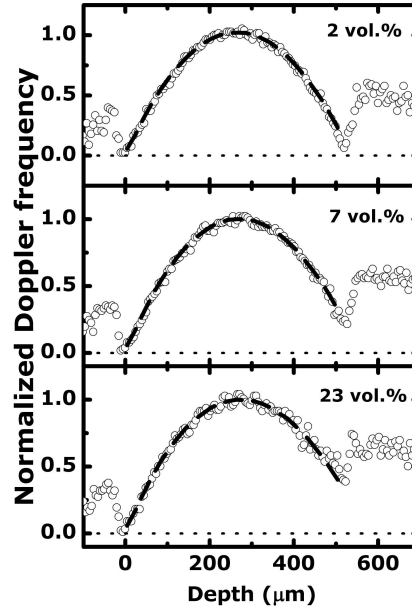


Fig. 8. Comparison between experimental Doppler OCT data from Fig. 4 (dots) and the MC simulations (dashed line) for three different Intralipid concentrations (indicated). The experimental and Monte Carlo Doppler data are normalized prior to comparison.

#### 4. Discussion

We performed a systematic study of OCT signal attenuation and the Doppler OCT signal in flowing Intralipid solutions with varying scattering strength.

##### 4.1 OCT signal attenuation

We showed the effect of Intralipid concentration on the single exponential decay of the OCT signal attenuation. From a comparison of our OCT measurements and MC simulations we conclude that for all Intralipid concentrations the single scattering coefficient  $\mu_s$  is 15% higher than the measured OCT signal attenuation rate due to multiple scattering effects. Consequently, the single scattering coefficient  $\mu_s$  versus Intralipid concentration shows a behavior similar to that in Fig. 3(b), but is 15% higher. Additional MC simulations by us (not shown) have revealed that the OCT signal attenuation slope depends also on the  $g$  factor. The 15% difference between the single scattering coefficient  $\mu_s$  and the measured OCT attenuation rate increases rapidly for  $g$  factors increasing from 0.33 to 1. An additional parameter effecting the OCT signal attenuation is the coherence length  $l_c$  of the source. An increase of the coherence length causes an increase of the number of multiple scattered photons in the OCT signal and thus leads to a decrease of the OCT signal slope. Therefore, the difference between the single scattering coefficient  $\mu_s$  and the measured OCT signal attenuation rate increases. However, the dependence on the coherence length in general is less strong than the dependence on the  $g$  factor. Therefore, for an accurate determination of the single scattering coefficient  $\mu_s$  in a medium with high  $g$  factor, multiple scattering has to be further suppressed by using a shorter coherence length, and/or a stronger confocal gate with focus tracking.

Our determination of the single scattering  $\mu_s$  clearly demonstrates, for the first time to our knowledge, the effect of concentration dependent scattering on the single scattering coefficient  $\mu_s$  measured with OCT. We attribute this non-linear increase to coherence effects of light scattered simultaneously from particles that are close together. For higher Intralipid concentrations the coherent addition of light results in a reduced amount of light that scatters out of the beam, thereby decreasing the optical attenuation in the medium. In other words, the scattering cross section in the high density medium decreases relative to the single particle (Mie) scattering cross section. This effect was already observed by Zaccanti et al. [11] in optical transmission measurements of Intralipid, but also has been investigated by many others, e.g. see Refs [10,22,23]. and references therein. Dependent scattering significantly reduces the scattering coefficient for high density media, thereby reducing multiple scattering effects and increasing the OCT imaging depth. In contrast to the linear extrapolation  $\mu_s = C\sigma_s$  that many people use for Intralipid [13] and other scattering media, one should be cautious in estimating the optical signal attenuation for high density media. The effect of dependent scattering is determined by the microscopic environment of the scatterers which can be quantified for well-defined model systems, such as monodisperse non-interacting spheres, but is difficult to quantify for biological systems where these effects will vary from position to position (depending on the microenvironment of the scatterer).

Note that we neglected any dependence of the scattering anisotropy  $g$  on the Intralipid concentration in our simulations. As shown by Zaccanti et al. [11] this effect is small and we expect it to be even smaller for  $g = 0.33$  at 1300 nm wavelength.

#### 4.2 Doppler OCT signal

Experimentally and with MC simulations, we have shown the effect of multiple scattering on the OCT signal attenuation slope and on the Doppler OCT flow in Intralipid. The fact that we get a consistent agreement between the simulations and the measurements for both OCT signal attenuation and Doppler OCT data supports the interpretation of our data. Multiple scattering influences flow parameters measured with Doppler OCT such as peak flow, peak flow location, flow volume, and shear rate. To accurately quantify these parameters from Doppler OCT measurements in highly scattering media, multiple scattering effects have to be taken into account.

Evidently, the main application for Doppler OCT are in-vivo blood flow measurements. For blood, the scattering rates are much higher than for Intralipid, thereby increasing multiple scattering effects. However, the scattering anisotropy is also much larger, and consequently, the Doppler frequency shift for a (multiple) forward scattering event is much smaller. From MC simulations for blood we have observed that multiple scattering effects on Doppler blood flow measurements can be significant, however, the precise magnitude of this effect is still to be determined experimentally.

### 5. Conclusion

This work describes the influence of both multiple and dependent scattering effects on the Doppler OCT signal in Intralipid. Although a good understanding of light scattering in high density media is very challenging, we do believe that with a correct analysis, either theoretical or with MC simulations, accurate quantitative tissue and flow parameters can be determined.

### Acknowledgments

J. Kalkman is supported by the IOP Photonic Devices program managed by the Technology Foundation STW and SenterNovem. D. J. Faber is funded by a personal grant in the Vernieuwingsimpuls program by the Netherlands Organization of Scientific Research (NWO) and the Technology Foundation STW (AGT07544). A. V. Bykov acknowledges the joint grant of Academy of Finland (appl. No124176) and Russian Foundation for Basic Research (No. 08-02-91760-AF\_a).